



Photoelectrochemical oxidation of organic substances over nanocrystalline titania: Optimization of the photoelectrochemical cell

Maria Antoniadou, Panagiotis Lianos*

University of Patras, Engineering Science Dept., 26500 Patras, Greece

ARTICLE INFO

Article history:

Available online 25 March 2009

Keywords:

Photoelectrochemical cell
Nanocrystalline titania
Photodegradation

ABSTRACT

The photocatalyzed oxidation of various organic substances has been studied in a two compartment, chemically biased photoelectrochemical cell. The organic substances studied were either derivatives of biomass and, generally, of natural products or they were potential water pollutants, like surfactants. The purpose of the study was the assessment of the feasibility of employing solar radiation to produce electricity with simultaneous water cleaning or consumption of surplus biomass derivatives. The study includes optimization of the photoelectrochemical cell by using different types of cathode electrodes and a standard nanocrystalline titania anode.

© 2009 Elsevier B.V. All rights reserved.

1. Introduction

Photocatalytic treatment of water wastes using nanocrystalline titania photocatalyst is a very popular research subject. In principle, photocatalytic treatment of water should lead to complete mineralization, i.e., in the case of organic wastes, production of carbon dioxide. There exist a vast number of works treating the question of photocatalytic efficiency for a large variety of organic targets. Most of the researchers concentrate on the question of efficiency and on the extent of mineralization. However, another important aspect of photocatalysis, concerning energy yield and energy conversion routes, is recently getting renewed interest. Most organic wastes are rich in hydrogen. Hydrogen ions may be produced during photocatalytic oxidation and, by interaction with dissolved oxygen, may produce water. This intermediate role of hydrogen is not noticed and it is neglected. However, under certain conditions, it is possible to reduce hydrogen ions and produce molecular hydrogen, which thus becomes a useful product of the photocatalytic process. There exist two main procedures to produce hydrogen by photocatalytic oxidation. In the so-called photocatalytic (PC) process, noble metal nanoparticles (usually Pt) are deposited on the titania nanocrystalline photocatalyst [1–11]. When photons are absorbed by the semiconductor, they generate electron–hole pairs. Holes oxidize the target substance, either directly or through OH[•] radical intermediates. Electrons, on the other hand, are trapped and

retained by the metal and they can reduce H⁺ to molecular hydrogen. This is directly accomplished in the aqueous solution of the target substance without any additives, other than the metal/semiconductor photocatalyst and it is considered a fairly efficient process. In the so-called photoelectrochemical (PEC) process, photooxidation is carried out in a photoelectrochemical cell [12–16]. The photoanode is made of an electrode, where nanocrystalline titania has been deposited. Typical substrate for this purpose is a transparent conductive glass electrode bearing a layer of tin-doped indium oxide (ITO) or fluorine-doped tin oxide (SnO₂:F) [16] or it may simply be a titanium foil [15]. The dark cathode can be made of many different materials, as will be discussed in the present work. Photooxidation of the target substance follows light absorption by the anode and occurs by means of the photo-generated holes. Photogenerated electrons move through an external circuit to the dark cathode, thanks to the existing potential difference. This difference can be enhanced in a two compartment cell by placing two different electrolytes in the two compartments, a basic electrolyte in the anode and an acidic electrolyte in the cathode compartment. Hydrogen ions generated during photooxidation move towards the cathode by diffusing through the electrolyte and they are reduced by the externally arriving electrons producing molecular hydrogen. Indeed, hydrogen is detected under anaerobic conditions, for example, by passing an inert gas through the cathode compartment [16]. Under aerobic conditions, hydrogen interacts with oxygen and produces water. In both cases, an electric current flows between the anode and the cathode. It is then possible to photooxidize an organic substance and produce electricity. This solar-to-electricity conversion, with or without hydrogen production, is a very attractive

* Corresponding author. Tel.: +30 2610 997513; fax: +30 2610 997803.
E-mail address: lianos@upatras.gr (P. Lianos).

idea, since it leads to water cleaning with energy yield. In the present work, we employ a chemically biased two compartment cell to study the PEC process.

PEC operation necessitates external flow of electrons and internal flow of hydrogen ions. The efficiency of the cell then depends on ionic conductivity, which is facilitated by adding electrolyte(s) in the reaction solution and by producing as many hydrogen ions as possible. Hydrogen ions can be produced simply by water oxidation but experience shows that this is a much less efficient process than organic substance oxidation [16]. Among the different organic substances so far tried, ethanol and glycerol, both products of biomass, are among the best materials for efficient PEC operation. In the present work, we use ethanol in comparison with other substances to study the efficiency of PEC operation. Photooxidation of ethanol in the presence of water is part of the photocatalytic reforming reaction [7]:



According to Eq. (1), photooxidation of ethanol during a PEC operation should lead to mineralization with CO_2 evolution at the photoanode and hydrogen evolution at the dark cathode. Of course, as already said, under aerobic conditions hydrogen interacts with oxygen and produces water. In the present work we focus attention on a PEC operation under aerobic conditions for both anode and cathode and we measure the electric characteristics of the cell. Therefore, the cell is exclusively employed to convert light into electricity by consuming organic material.

A light-to-electricity conversion device depends on the quality of both the anode and the cathode. In the present work, a standard anode is being used but special attention is being paid on the cathode materials and on their optimization for increasing cell efficiency.

2. Experimental

2.1. Materials

The nanocrystalline titania used in the present work was commercial Degussa P25, which consists of 25–30 nm nano-

particles. All the other reagents were from Aldrich and Merck, while Millipore water was used in all experiments. $\text{SnO}_2:\text{F}$ transparent electrodes (resistance $8 \Omega/\text{sq}$) were purchased from Hartford, USA. Nafion membrane was purchased from Ion Power, Inc., USA.

2.2. Deposition of titania films

Nanocrystalline Degussa P25 was dispersed in a mixture of water, ethanol and polyethyleneglycol (PEG) 2000 as in a previous publication [16]. Briefly, 0.3 g of Degussa P25 was dispersed by vigorous stirring in 3 ml of a solution made of about 10 ml water, 10 ml of ethanol and 1 g of PEG 2000. The resulting material was a white paste, which can be easily cast on any solid substrate. Films were thus made by casting the paste on $\text{SnO}_2:\text{F}$ transparent electrodes. After casting, the electrodes were calcined at 550°C . This relatively high temperature was necessary to assure that all organic templates were destroyed. High calcination temperature adversely affects the conductivity of the transparent conductive electrode. This problem is less pronounced when $\text{SnO}_2:\text{F}$ are used, as in the present case (compared, for example, to indium-tin-oxide (ITO), electrodes). The procedure was repeated once more. The final quantity of titania on the electrode was 25 mg, while the dimensions of the film was $4 \times 2.5 = 10 \text{ cm}^2$. Thanks to the high calcination temperature, the film adhered well on the $\text{SnO}_2:\text{F}$ electrode and withstood the hard alkaline conditions during cell operation. Fig. 1a shows a picture of such an electrode with applied film and wire connection. The latter was made by using an auto adhesive copper ribbon.

2.3. Construction of the cathode

Various electrodes were used as cathode in the present work. Platinized platinum electrode was prepared by casting an aqueous solution of about $10^{-3} \text{ mol L}^{-1} \text{ Na}_2\text{PtCl}_4 \cdot x\text{H}_2\text{O}$ on a $2 \text{ cm} \times 2 \text{ cm}$ platinum foil. Then it was washed and heated in the air at 500°C . Deposition of platinum nanoparticles on a platinum foil aims at increasing the active surface area of the electrode. A series of electrodes was also prepared by depositing various metal nanoparticles on $\text{TiO}_2/\text{SnO}_2:\text{F}$ electrodes identically structured as the anode electrode. A solution of about $10^{-3} \text{ mol L}^{-1}$ of one of the

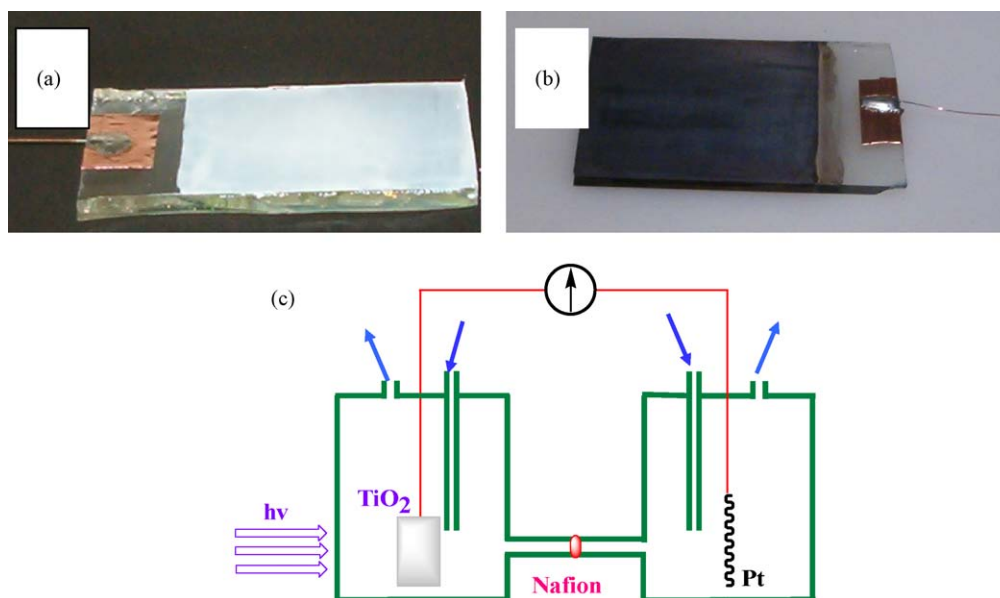


Fig. 1. (a) Photograph of the anode assembly depicting transparent conductive electrode, titania film and wire connection; (b) photograph of the cathode assembly depicting transparent conductive electrode, titania film, adsorbed Pt and wire connection; (c) schematic representation of the H-shaped PEC reactor.

following metal salts: $\text{Na}_2\text{PtCl}_4 \cdot x\text{H}_2\text{O}$; $\text{Na}_2\text{AuCl}_4 \cdot 2\text{H}_2\text{O}$; AgNO_3 ; $\text{Na}_2\text{PdCl}_4 \cdot x\text{H}_2\text{O}$; and $\text{NiC}_2\text{H}_4\text{O}_2 \cdot 4\text{H}_2\text{O}$ was cast on the surface of a $\text{TiO}_2/\text{SnO}_2:\text{F}$ electrode, freshly prepared as in the previous paragraph. Then it was heated in air at 500°C to assure reduction of adsorbed Pt(II) to metallic Pt. The procedure was repeated two more times so that the surface of the electrode became deeply dark as in the example depicted in the photograph of Fig. 1b. In one case, we cast $\text{Na}_2\text{PtCl}_4 \cdot x\text{H}_2\text{O}$ solution on a plain $\text{SnO}_2:\text{F}$ electrode, not bearing a titania film, in the same way as when it bore one. Also some preliminary experiments were made by using a Pt-loaded carbon cloth prepared as in Ref. [17].

2.4. Structure of the reactor

The PEC cell was a two compartment (H-shaped) reactor made of Pyrex glass, schematically shown in Fig. 1c. Appropriate tubing allowed carrier gas to be introduced in each compartment. The anode was made of one single $\text{SnO}_2:\text{F}$ electrode with deposited nanocrystalline titania (cf. Fig. 1a), while the cathode was one of the electrodes described in the previous paragraph (for example, that of Fig. 1b). The electrolyte of the anode compartment contained 1.0 mol L^{-1} NaOH and that of the cathode contained 1.0 mol L^{-1} H_2SO_4 . The electrolyte concentrations were optimized in a previous publication [16] and were similar with those used in Ref. [15]. The Nafion membrane separating the two compartments of the cell was activated by the following procedure: a piece of about 2 cm diameter was cut from a larger sheet (Ion Power, N-117, $183\ \mu\text{m}$ thick) and was submerged in a 0.1 mol L^{-1} aqueous solution of H_2O_2 at 80°C for 1 h. Then it was submerged for 1 h at 80°C in pure water followed by 1 h at 80°C in 0.1 mol L^{-1} H_2SO_4 and finally for 1 more hour at 80°C in pure water. After this procedure, it was stored at ambient temperature in pure water. The active section of the membrane, when mounted on the reactor, had a diameter of about 1 cm. Exciting radiation was generated by a homemade source employing Black Light tubes with spectral maximum around 360 nm. These tubes provide band gap excitation of titania, as it is explained in previous publications [10,11]. Four tubes of 4 W nominal (electric) power were symmetrically placed inside a cylindrical cavity with reflective wall. A slit in the reflective wall was cut to allow introduction of the cell, so that only the anode compartment was maintained inside the cavity and the rest was outside. The intensity of radiation at the position of the film and by facing a Black Light tube was 0.80 mW cm^{-2} . Since there were 4 tubes located around the anode compartment and since the film support was transparent, we accepted that the total UVA radiation incident on the photocatalyst was equal to $4 \times 0.8 = 3.2\text{ mW cm}^{-2}$.

2.5. Apparatus

The intensity of radiation at the position of the catalyst was measured with an Oriol Radiant Power Meter. Electrical measurements were made with a Keithley 196 multimeter while IV scans were recorded with a computerized Keithley 2601 source meter. Detection of hydrogen was made online by using an SRI 8610C gas-chromatograph and Ar as carrier gas, similarly to previous publications [10,11,16].

3. Results and discussion

Most of the experiments described in this work were made by loading the PEC cell with a water ethanol mixture, which is among the best choices for a PEC operation. The high efficiencies obtained in the presence of ethanol are demonstrated by the data of the following paragraph.

3.1. Current–voltage characteristics and efficiencies of PEC cells functioning with different organic loads

An H-shaped two compartment cell, like the one of Fig. 1c, was used for all experiments. The two compartments were separated by a Nafion membrane as described in Section 2.4. The anode compartment contained an aqueous solution of the organic photodegradable substance and 1.0 mol L^{-1} NaOH. The cathode compartment contained only the acidic electrolyte made of 1.0 mol L^{-1} H_2SO_4 . These electrolytes create highly acidic or basic environments, which might make electrodes vulnerable to corrosion. However, we have detected no signs of deterioration of the presently used electrodes, at least, within the duration of the experiments. A Pt/ $\text{TiO}_2/\text{SnO}_2:\text{F}$ (cf. Fig. 1b) was employed as cathode. The currents observed under UVA illumination, which provides band gap excitation of the titania photoanode [10,11], are expressed in mA cm^{-2} , that is, as current density, as it is the usual practice. The values of the current density were calculated by dividing the measured current by the surface of the titania film, which, as already said, was 10 cm^2 . This is not the safest way to calculate current density since it gives underestimated values. The proper way is to construct electrodes bearing titania films of small surface area [18,19]. Such size reduction presents some practical difficulties and for this reason we employed relatively large films by overlooking this point and the ensuing error, which is not crucial for the present work. Thus the values of the measured current can be directly recovered in mA by multiplying J_{sc} values by 10. When pure water was used in both anode and cathode compartments, the measured current was practically zero both in the dark and under illumination. The presence of electrolyte was then necessary to detect any current at all. Optimization of the electrolyte concentration was done in a previous publication [16]. Dark currents were practically zero in all studied cases in this work. Table 1 lists the values of the short-circuit current density J_{sc} , the open-circuit voltage V_{oc} , the fill factor (ff) and the overall efficiency

Table 1

Cell current–voltage characteristics under UVA (Black Light) illumination for various reactants in the anode compartment. The anode compartment also contained 1.0 mol L^{-1} aqueous NaOH and the cathode compartment contained 1.0 mol L^{-1} aqueous H_2SO_4 .

| Reactant and its concentration | J_{sc} (mA cm^{-2}) | V_{oc} (mV) | ff | η (%) |
|--|---|----------------------|------|------------|
| Pure water without any additives besides electrolyte | 0.11 | 1400 | 0.19 | 0.9 |
| Alcohols | | | | |
| MeOH (20%v.) | 1.12 | 1650 | 0.19 | 10.9 |
| EtOH (20%v.) | 1.03 | 1670 | 0.18 | 9.2 |
| PrOH (20%v.) | 1.00 | 1650 | 0.16 | 8.0 |
| Polyols and sugars | | | | |
| Glycerol (20%v.) | 1.12 | 1790 | 0.17 | 10.5 |
| Xylitol (0.063 mol L^{-1}) ^a | 0.78 | 1810 | 0.16 | 7.2 |
| Sorbitol (0.052 mol L^{-1}) ^a | 0.96 | 1730 | 0.14 | 7.1 |
| Glucose (0.048 mol L^{-1}) ^a | 0.45 | 1790 | 0.22 | 5.6 |
| Fructose (0.053 mol L^{-1}) ^a | 0.27 | 1770 | 0.21 | 4.7 |
| Lactose (0.028 mol L^{-1}) ^a | 0.42 | 1720 | 0.21 | 4.8 |
| Various water pollutants | | | | |
| Ammonia (1%v.) ^b | 0.44 | 1580 | 0.27 | 5.9 |
| Urea (0.83 mol L^{-1}) | 0.20 | 1570 | 0.29 | 3.8 |
| Triton X-100(2%v.) ^c | 0.19 | 1710 | 0.26 | 5.9 |
| SDS (0.033 mol L^{-1}) ^d | 0.49 | 1210 | 0.27 | 5.8 |
| CTAB (0.033 mol L^{-1}) ^e | 0.24 | 1500 | 0.26 | 2.9 |
| Dish-wash detergent (1%v.) ^f | 0.35 | 1610 | 0.24 | 4.2 |

^a The corresponding quantity in grams was 9.5 g L^{-1} .

^b Obtained by dilution of a 25% ammonia solution.

^c A non-ionic surfactant: polyoxyethylene-(10) isoctylphenyl ether.

^d An ionic surfactant: sodium dodecylsulfate.

^e A cationic surfactant: cetyltrimethylammonium bromide.

^f Commercial dish-wash detergent under the brand name AVA.

of the cell. The fill factor is a quantity given by the following equation:

$$ff = \frac{JV_{\max}}{J_{sc}V_{oc}} \quad (2)$$

where JV_{\max} is the maximum value of the JV product, as extracted from JV plots (cf. Fig. 2). The fill factor then gives the extent of diversion between the actual maximum power density that can be produced by the cell and the product $J_{sc}V_{oc}$, that is, the product of the highest possible values of current density and voltage. The quality of a cell is directly related with its fill factor, the optimized value of which should be as high as possible. The efficiency of the cell in the present case was calculated by using the following formula:

$$\eta = \frac{JV_{\max}}{P} \quad (3)$$

By definition (see also Ref. [16]), η is the ratio of the actual maximum power produced by the cell over the incident light power P , i.e., 3.2 mW cm^{-2} , in the present case.

The data of Table 1 were obtained under aerobic conditions for both the cathode and the anode compartment. However, some experiments were also made by passing Ar through the cathode compartment. In that case hydrogen was detected and measured by a gas-chromatograph, as in a previous publication [16]. Table 1 shows that pure electrolyte without any organic additive gave the smallest open-circuit voltage and the smallest short-circuit current density and cell efficiency. It is then once more demonstrated that water oxidation by itself is not a very efficient process. The highest efficiency was calculated in the case of MeOH and glycerol followed by ethanol. Since it is practically easy to employ ethanol, this substance was chosen for the rest of the experiments. Table 1 lists a representative choice of substances that may be found in water wastes or they are abundant materials

derived from biomass and generally from natural products. Especially, in the case of glycerol, a surplus is expected, since this substance is a byproduct of bio-diesel production [20]. In addition to ethanol and glycerol, which are typical biomass derivatives, Table 1 lists data obtained with other alcohols, polyols and sugars (see Table 2), human wastes like urea and ammonia, three known synthetic surfactants, i.e., a non-ionic (Triton X-100), an ionic (SDS) and a cationic (CTAB), and a common dish-wash surfactant material. Among the group of alcohols, the shortest chain length methanol gave the highest performance. Also among the group of polyols and sugars, whose chemical structure is shown in Table 2, glycerol gave the highest efficiency. Longer chain analogs gave smaller efficiencies while sugars demonstrated even smaller performance. It seems then that smaller molecules are more performing than larger ones. This result is probably due to the fact that longer molecules necessitate more oxidative steps to achieve complete reforming and mineralization, as in Eq. (1). The cell efficiencies listed in Table 1 are relatively large. The reason is that the exciting radiation has a limited spectral extent around 360 nm and it is directly absorbed by titania with small losses. The data of Table 1 reveal that the above electrochemical cell can be successfully employed to photodegrade a large variety of water pollutants as well as water soluble surplus material derived from biomass, leading to water cleaning with simultaneous production of electricity. Practical applications of the above procedure are then feasible. The next issue that naturally emerges from this conclusion is to construct PEC cells with optimized efficiency. This matter is treated in the next paragraph.

3.2. Optimization of a photoelectrochemical cell functioning in the presence of ethanol

As already said, ethanol is a good choice for a material filling a PEC reactor since it offers high efficiency, it is easy to obtain and

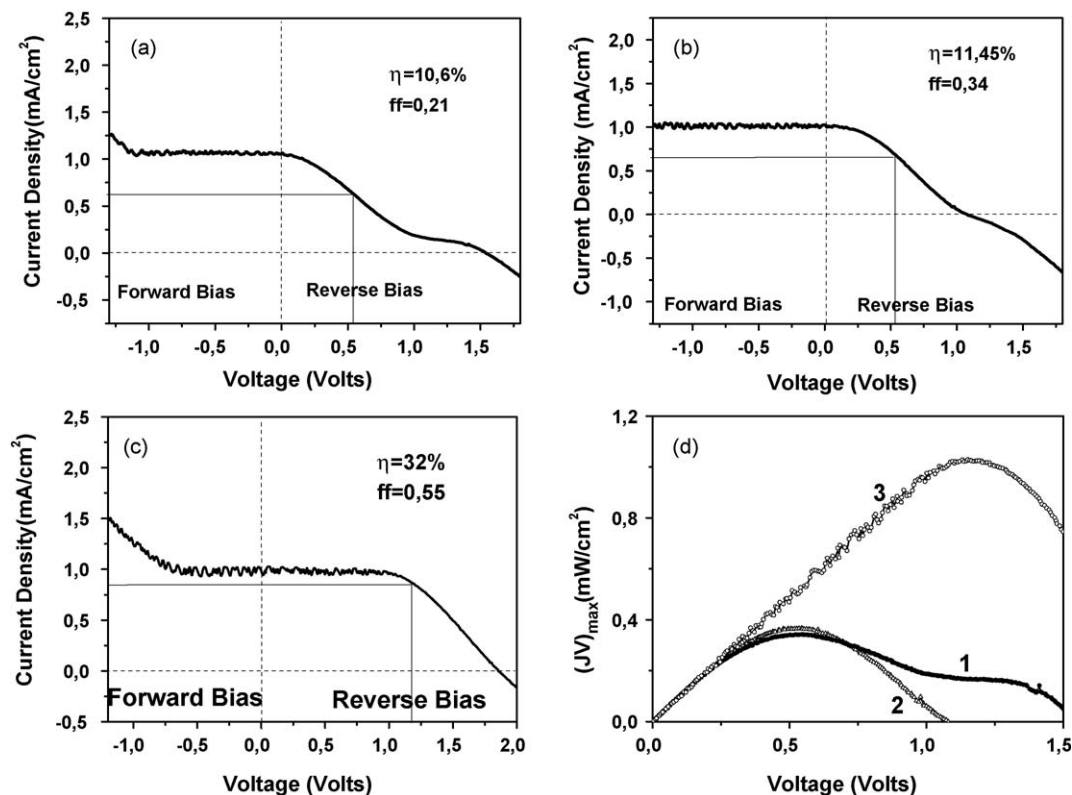
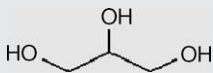
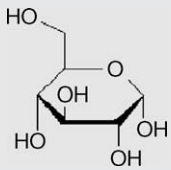
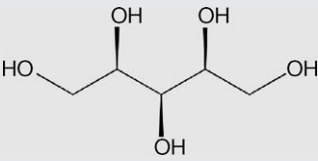
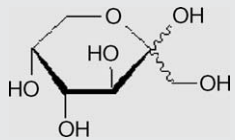
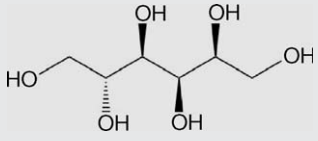
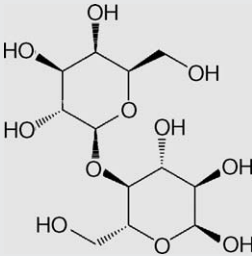


Fig. 2. JV plots for cell operation with three different cathode electrodes: (a) $\text{Ag}/\text{TiO}_2/\text{SnO}_2:\text{F}$; (b) platinumized platinum foil; (c) platinum-loaded carbon cloth; and (d) JV vs. V plots for the data corresponding to the plots: (1) a; (2) b; (3) c.

Table 2
Chemical structures of some carbohydrates studied in this work.

| Name | Chemical structure | Name | Chemical structure |
|----------|---|----------|---|
| Glycerol |  | Glucose |  |
| Xylitol |  | Fructose |  |
| Sorbitol |  | Lactose |  |

non-toxic to use. The percentage of ethanol necessary to introduce into the water–ethanol mixtures filling the anode compartment has been studied in a previous publication [16]. It was concluded that 20%v. ethanol is a good choice for optimal results. In the present paragraph, we study the electrical characteristics of a two compartment PEC cell, employing 20%v. ethanol/water mixtures, a standard anode, as the one described in Section 2.2 and used so far, and a variety of cathodes. As it will be shown below, the quality of the cathode had a strong influence on cell efficiency. Table 3 presents JV values and the efficiency of cells made with various cathodes. J_{sc} , V_{oc} and JV_{max} , necessary for efficiency calculations by means of Eq. (2), were extracted from plots like the ones of Fig. 2. JV_{max} is the maximum $J \times V$ product. The position and the value of JV_{max} can be calculated by plotting the value of the $J \times V$ product versus, for example, the value of V , as in Fig. 2d. The position of JV_{max} is shown in Fig. 2a–c by the vertical lines. The fill factors were then calculated according to Eq. (2), as above. Inspection of Table 3 reveals the following: the values of the short-circuit current density J_{sc} were practically very close to each other and did not substantially depend on the type of the cathode, except in the case of the Ni/TiO₂/SnO₂:F electrode. This type of cathode gave much lower performance than any other case studied. The uniformity of current density is most probably due to the standard geometry of the cell, the size of the Nafion membrane, the geometry of the electrodes and the ionic conductivity of the filling electrolyte, which set upper limits to current flow. The marked decrease of current in the case of Ni/TiO₂/SnO₂:F is obviously due to the limited ability of Ni to catalyze reduction process at the cathode. On the contrary, open-circuit voltage V_{oc} demonstrated a large variation from one type of cathode to another. No specific tendency for V_{oc} could be, however, detected. V_{oc} values of both Tables 1 and 3, were generally high. This is due to the presence of chemical bias in addition to the intrinsic potential difference between the semiconductor and the metal electrode. Indeed, the potential difference dictated by the different electrolytes in the two cell compartments, according to the rule $\Delta V = 0.059 \Delta pH$ [12,16] is

expected to add 732 mV [16] to the value of V_{oc} . The highest V_{oc} value was registered in the case of Pt loaded carbon cloth (Pt/CC). The clearest picture of the quality of the cathode is given by the value of the fill factor. A platinized platinum electrode had a higher fill factor than a plain platinum electrode. This is expected, since the addition of platinum nanoparticles increased the active surface area of the electrode. Comparable or even higher fill factors were measured in the case of some electrodes made by depositing noble metals on TiO₂/SnO₂:F electrodes. Only Pt and Pd offered this quality, while Au, Ag and Ni gave much lower fill factors. It is then concluded that TiO₂/SnO₂:F electrodes with deposited Pt or Pd nanoparticles, which are easy to make, can well substitute for platinum electrodes, which are more expensive to obtain. The role of the nanocrystalline titania substrate in this case is to adsorb and stabilize metal nanoparticles. Thus in the absence of titania (4th row of Table 3) the fill factor was much lower. The size and distribution of metal nanoparticles on the TiO₂/SnO₂:F cathode is a

Table 3
Cell current–voltage characteristics under UVA (Black Light) illumination for various cathode electrodes. The anode compartment contained a 20%v. ethanol/water mixture and 1.0 mol L⁻¹ aqueous NaOH and the cathode compartment contained 1.0 mol L⁻¹ aqueous H₂SO₄.

| Type of cathode | J_{sc} (mA cm ⁻²) | V_{oc} (mV) | ff | η (%) |
|--|---------------------------------|---------------|------|------------|
| Platinum electrodes | | | | |
| Platinum wire | 1.13 | 1160 | 0.19 | 7.7 |
| Non-platinized platinum foil | 1.12 | 840 | 0.28 | 8.2 |
| Platinized platinum foil | 1.10 | 1060 | 0.34 | 12.4 |
| Platinized SnO ₂ :F electrode | 1.15 | 1430 | 0.24 | 12.3 |
| Metal nanoparticles deposited on a TiO ₂ /SnO ₂ :F electrode | | | | |
| Pt/TiO ₂ /SnO ₂ :F | 1.11 | 1080 | 0.33 | 12.4 |
| Pd/TiO ₂ /SnO ₂ :F | 1.05 | 1060 | 0.37 | 12.9 |
| Au/TiO ₂ /SnO ₂ :F | 1.03 | 1330 | 0.26 | 11.1 |
| Ag/TiO ₂ /SnO ₂ :F | 1.06 | 1530 | 0.21 | 10.6 |
| Ni/TiO ₂ /SnO ₂ :F | 0.77 | 1190 | 0.20 | 5.7 |
| Platinum-loaded carbon cloth | 1.01 | 1860 | 0.55 | 32.3 |

subject of current research in our laboratory. The results will be presented in a future publication. An impressively higher fill factor value was calculated in the case of Pt/CC cathode. In order to obtain an idea of what means for a cell to have a high fill factor and to explain how the various data of Tables 1 and 3 were extracted, Fig. 2 presents JV plots for three characteristic cases of very low, average and highest ff value. Perpendicular lines on each plot mark the position of the JV_{\max} and the values of J_{sc} and V_{oc} . Each plot is a measure of the current density under various values of forward or reverse bias (voltage) applied between the two electrodes. It is noted that as the fill factor increases, the area below the reverse bias plot increases. The plateau formed by the plot moves more and more into the reverse bias space as ff increases. This means that a cell with high fill factor has a higher ability to preserve its current under increasing reverse bias. This, in turn, is due to the high reduction capacity of such a cathode that facilitates electron flow. Apparently, Pt/TiO₂/SnO₂:F and Pd/TiO₂/SnO₂:F electrodes demonstrate a good performance but Pt/CC electrodes are by far the most performing. The superior performance of Pt/CC electrodes is due to their high load in Pt nanoparticles, in analogy with the high performance of the Pt/TiO₂/SnO₂:F electrode also loaded with a lot of Pt nanoparticles. Pt/CC electrodes can be found in many varieties, both commercial and home made. The example of Table 3 is neither unique nor the most representative. Cell performance by using various Pt/CC cathodes are currently under study in our laboratory and the results will be presented in a future publication. The last column of Table 3, gives the overall cell performance under UVA radiation. The most efficient cells were again those made with Pt/CC cathodes. The above data and discussion are very useful in designing high-performing cells.

The present PEC cell was run with low power Black Light radiation providing about 3.2 mW cm⁻² light intensity. This value is comparable with the intensity of the UVA part of the solar noon. Therefore, the above PEC cell can be run by using solar radiation. Indeed, our cells were used outdoors under solar illumination and offered comparable results as those analyzed above.

The data presented in Tables 1 and 3 correspond to experiments made with fresh solutions. As the oxidation went on, the value of the current decreased. One reason for such a decrease is the consumption of the target organic substance. However, there are also other reasons related with the kind of byproducts been created during the oxidation process and the number of steps necessary to achieve complete mineralization in each case. This matter is subject of current research in our laboratory.

4. Conclusions

A chemically biased two-electrode two compartment photoelectrochemical cell can be employed to photodegrade various

water soluble substances and produce electricity by using low power artificial light sources or solar radiation. Chemical bias was obtained by dissolving a basic electrolyte in the anode and an acidic electrolyte in the cathode compartment. A broad variety of organic substances, i.e., short chain alcohols, polyols, sugars and potential water pollutants were photocatalytically oxidized in the cell producing electricity. Methanol and glycerol, followed by ethanol, offered the highest cell performance. However, satisfactory performance was obtained with all studied substances. A PEC cell then can be used to clean water and produce electricity at the expense of artificial or solar light. Performance of the cell can be improved by optimizing cathode. Best cathodes are those made of Pt/CC electrodes but satisfactory performance was also obtained with noble metal loaded nanoporous titania electrodes.

Acknowledgements

We are grateful to Dr. S.G. Neophytides, FORTH/ICE-HT, Patras, for donating the Pt loaded carbon cloth electrodes and for useful discussions concerning this work. Financial support from the Program PENED (03EΔ607) of the General Secretariat of Research and Technology Hellas is graciously acknowledged.

References

- [1] T. Sakata, T. Kawai, Chem. Phys. Lett. 80 (1981) 341.
- [2] T. Miyao, Y. Suzuki, S. Naito, Catal. Lett. 66 (2000) 197.
- [3] M.C. Blount, J.A. Buchholz, J.L. Falconer, J. Catal. 197 (2001) 303.
- [4] A. Galinska, J. Walendziewski, Energy Fuels 19 (2005) 1143.
- [5] A. Patsoura, D.I. Kondarides, X.E. Verykios, Appl. Catal. B: Environ. 64 (2006) 171.
- [6] Y. Mizukoshi, Y. Marisa, T. Shuto, J. Hu, A. Tominaga, S. Shironita, S. Tanabe, Ultrason. Sonochem. 14 (2007) 387.
- [7] A. Patsoura, D.I. Kondarides, X.E. Verykios, Catal. Today 124 (2007) 94.
- [8] L.S. Al-Mazroai, M. Bowker, P. Davies, A. Dickinson, J. Greaves, D. James, L. Millard, Catal. Today 122 (2007) 46.
- [9] D.I. Kondarides, V.M. Daskalaki, A. Patsoura, X.E. Verykios, Catal. Lett. 122 (2008) 26.
- [10] N. Strataki, V. Bekiari, D.I. Kondarides, P. Lianos, Appl. Catal. B: Environ. 77 (2007) 184.
- [11] N. Strataki, P. Lianos, J. Adv. Oxid. Technol. 11 (2008) 111.
- [12] T. Bak, J. Nowotny, M. Rekas, C.C. Sorrell, Int. J. Hydrogen Energy 27 (2002) 991.
- [13] G. Milczarek, A. Kasuya, S. Mamykin, T. Arai, K. Shinoda, K. Tohji, Int. J. Hydrogen Energy 28 (2003) 919.
- [14] J. Nowotny, C.C. Sorrell, L.R. Sheppard, T. Bak, Int. J. Hydrogen Energy 30 (2005) 521.
- [15] M. Kitano, M. Takeuchi, M. Matsuoka, J.M. Thomas, M. Anpo, Catal. Today 120 (2007) 133.
- [16] M. Antoniadou, P. Bouras, N. Strataki, P. Lianos, Int. J. Hydrogen Energy 33 (2008) 5045.
- [17] I.D. Raistrick, U.S. Patent 4,876,115 (1989).
- [18] P.R. Mishra, P.K. Shukla, O.N. Shrivastava, Int. J. Hydrogen Energy 32 (2007) 1680.
- [19] P.R. Mishra, P.K. Shukla, A.K. Singh, O.N. Shrivastava, Int. J. Hydrogen Energy 28 (2003) 1089.
- [20] M. Pagliaro, R. Ciriminna, H. Kimura, M. Rossi, C. Della Pina, Angew. Chem. Int. Ed. 46 (2007) 4434.